Published in final edited form as:
Langmuir. 2012 May 29; 28(21): 8174–8182. doi:10.1021/la301094h.

Lipid Bilayers Covalently Anchored to Carbon Nanotubes

Yasaman Dayani and **Noah Malmstadt***
Mork Family Department of Chemical Engineering and Materials Science, University of Southern California, Los Angeles, California 90089, United States

Abstract

The unique physical and electrical properties of carbon nanotubes make them an exciting material for applications in various fields such as bioelectronics and biosensing. Due to the poor water solubility of carbon nanotubes, functionalization for such applications has been a challenge. Of particular need are functionalization methods for integrating carbon nanotubes with biomolecules and constructing novel hybrid nanostructures for bionanoelectronic applications. We present a novel method for the fabrication of dispersible, biocompatible carbon nanotube-based materials. Multi-walled carbon nanotubes (MWCNTs) are covalently modified with primary amine-bearing phospholipids in a carbodiimide-activated reaction. These modified carbon nanotubes have good dispersibility in nonpolar solvents. Fourier transform infrared (FTIR) spectroscopy shows peaks attributable to the formation of amide bonds between lipids and the nanotube surface. Simple sonication of lipid-modified nanotubes with other lipid molecules leads to the formation of a uniform lipid bilayer coating the nanotubes. These bilayer-coated nanotubes are highly dispersible and stable in aqueous solution. Confocal fluorescence microscopy shows labeled lipids on the surface of bilayer-modified nanotubes. Transmission electron microscopy (TEM) shows the morphology of dispersed bilayer-coated MWCNTs. Fluorescence quenching of lipid-coated MWCNTs confirms the bilayer configuration of the lipids on the nanotube surface and fluorescence anisotropy measurements show that the bilayer is fluid above the gel-to-liquid transition temperature. The membrane protein α-hemolysin spontaneously inserts into the MWCNT-supported bilayer, confirming the biomimetic membrane structure. These biomimetic nanostructures are a promising platform for the integration of carbon nanotube-based materials with biomolecules.

INTRODUCTION

Carbon nanotubes (CNTs) have received significant attention because of their unique structural, physical and electrical properties.[1–4] They have a wide range of applications in biosensing; gene and drug delivery in cells; intracellular transport of olignucleotides, proteins and peptides; biophysical studies; and nanodevices.[5–13] However, the hydrophobic surface of CNTs and their resulting insolubility in water limits their potential biomolecular applications. Carbon nanotubes have a tendency to aggregate in most solvents, leading to difficult-to-disperse bundles. Hydrophobic CNTs do not provide an appropriate environment for integration of biomolecules such as proteins, and they are highly resistant to any coupling with biomolecules.[14, 15] Here, we address these issues by fabricating a novel lipid-nanotube bioconjugate system in which lipid bilayers are covalently anchored to the surfaces of multi-walled carbon nanotubes (MWCNTs) to support the insertion of membrane proteins. This approach will not only facilitate the integration of CNTs with other

*Corresponding Author: Phone: (213)821-2034. Fax: (213)740-1056. malmstad@usc.edu. Address: 925 Bloom Walk, HED 216, Los Angeles, CA 90089.

biomolecules, but also establish a biocompatible platform for molecular devices and nanoscale architectures.

Several approaches have been developed for functionalization and solubilization of carbon nanotubes, including covalent and non-covalent surface modifications. Non-covalent functionalization has been based on surface adsorption of surfactants, polymers and biomolecules to CNTs and formation of CNT adduct nanostructures, such as CNT-crown ethers, using attractive electrostatic forces.[16–22] Covalent modifications involve direct reaction of CNTs to decorate their side walls with a desired functional group.[23–30] Many of the functionalization reactions are based on amiditaion and esterification of carboxylic acid-activated CNTs.[31] Although many covalent modifications allow for attachment of biomolecules to 1D nanomaterials, they offer a limited capacity to orient biomolecules and provide a biomimetic environment that facilitates biomolecular function.[32] Lipid bilayers attached to CNT surfaces can serve as a biomimetic environment for incorporating functional membrane proteins and other biomolecules.

To date, noncovalent modification of CNTs with single-tailed, double-tailed, dextran-containing phospholipids and polymerized lipids has been reported.[4, 33–37] Due to the amphiphilic nature of lipid molecules, they can self-assemble on the hydrophobic surface of CNTs in aqueous solution and provide a soluble supermolecular structure with wide range of applications.[33–35, 37] Although adsorption of lipids to CNTs leads to soluble, stable aqueous suspensions, the structures thereby formed lack the biomimetic structure of a true lipid bilayer. Direct self-assembly of lipid molecules on hydrophobic nanotubes instead forms a lipid monolayer.[4]

Several routes to the surface modification of CNTs with lipid bilayers have been proposed. Artyukhin et al. modified single-walled carbon nanotubes (SWCNT) with polyelectrolyte multilayers to make a hydrophilic polymer surface for lipid self-assembly.[1, 14] This modified SWCNT was incubated with lipid vesicles containing anionic and zwitterionic lipids leading to spontaneous bilayer formation by vesicle fusion.[14, 38] In other approaches lipid bilayers were formed on the hydrophilized surface of SWCNTs through fusion of small or giant vesicles.[15, 39–41] Self-assembly of bilayers on the hydrophilic surface of MWCNTs was also reported by Ye et al.[42] There have also been studies attempting covalent lipid modification of both SWCNTs and MWCNTs resulting in improved aqueous dispersion;[43, 44] however, these reports do not describe the formation of well characterized bilayers.

The covalent modification of CNTs provides an advantage over other methods in that it allows for durable attachment with higher stability.[23, 45] Such structures should be robust to changes in environmental conditions such as pH and temperature.

In this study, we introduce a novel approach for lipid bilayer formation on MWCNTs. MWCNTs have outer diameters in the range of 20–30 nm, providing a sufficiently large radius of curvature to allow for assembly of true molecular bilayers.[14, 46] Bilayer-coated MWCNTs were fabricated in a two-step process. First, lipid head groups were attached to the nanotube surfaces in a carbodiimide-mediated reaction. This creates a covalently modified nanotube surface that allows for the self-assembly of second lipid layer in a simple sonication process. The bilayer-coated MWCNT suspension is well dispersed and is stable for at least 60 days. The biomimetic cell membrane-like structure of the bilayer on the nanotube surface is demonstrated by the stable insertion of the bacterial membrane protein α-hemolysin[47–49], fluorescence quenching of dye-labeled lipid, and fluorescence anisotropy measurements of bilayer fluidity. These biocompatible carbon nanotubes will allow for the creation of novel nanoscale structures for biosensing and bioelectronics.

EXPERIMENTAL SECTION

Materials

COOH-functionalized multi-walled carbon nanotubes were obtained from Nanostructured and Amorphous Materials (Houston, TX, USA). 1,2-dipalmitoyl-*sn*-glycero-3-phosphoethanolamine (DPPE), 1-palmitoyl-2-{6-[(7-nitro-2-1,3-benzoxadiazol-4-yl)amino]hexanoyl}-*sn*-glycero-3-phosphocholine (NBD-PC), 1,2-dipalmitoyl-*sn*-glycero-3-phosphoethanolamine-N-(7-nitro-2-1,3-benzoxadiazol-4-yl) (NBD-PE), 1-palmitoyl-2-hydroxy-*sn*-glycero-3-phosphocholine (lyso-PC) and 1,2-dipalmitoyl-*sn*-glycero-3-phosphocholine (DPPC) were purchased from Avanti Polar Lipids (Alabaster, AL, USA). *N, N′*-diisopropylcarbodiimide (DIC), N-Hydroxysuccinimide (NHS), 5(6)-carboxytetramethylrhodamine N-succinimidyl ester (NHS-rhodamine), Triton X-100, sodium dodecyl sulfate (SDS), sodium hydrosulfite (sodium dithionite) and all solvents were from Sigma-Aldrich (St. Louis, MO, USA). Sodium bicarbonate and sodium chloride were obtained from J.T. Baker (Phillipsburg, NJ, USA). Sodium phosphate was from EMD chemicals (Gibbstown, NJ, USA).

Synthesis of Lipid-modified Multi-walled Carbon Nanotubes

For covalent conjugation of carbon nanotubes to DPPE, 1 mg of COOH-functionalized MWCNTs was suspended in 2 mL of a 2:1:1 (volume ratio) mixture of DMF, chloroform, and methanol and sonicated for 1 h. 10 mg DPPE along with a 10× molar excess NHS and 10× molar excess DIC as activator were added to the reaction mixture, sonicated for 1 h and stirred for 48 h at 50°C. The reaction mixture was centrifuged for 20 min at 4000 rpm to separate MWCNTs and remove unbound lipid molecules. The resulting supernatant was discarded and modified MWCNTs were washed with 1:1 (volume ratio) mixture of chloroform and methanol 3 times to remove free lipids. For complete removal of physisorbed lipids from the MWCNT surface, a 2% solution of triton X-100 in water was added to the MWCNTs, mixed thoroughly, and centrifuged for 15 min at 4000 rpm to pellet the MWCNTs. To remove any trace of detergent, MWCNTs obtained from this process were washed with pure water and centrifuged to pellet (4000 rpm, 15 min) 3 times. Then, a mixture of 1:1 chloroform and methanol was added to MWCNTs, mixed well and centrifuged for 2 more cycles. Lipid modified-MWCNTs were dried in vacuum overnight at 30 °C. As a control for physisorption, 1 mg COOH-functionalized MWCNTs were mixed with 10 mg DPPE in the absence of DIC and NHS. Otherwise all reacton and washing conditions were as applied in the synthesis of lipid-modified MWCNTs.

FTIR Analysis

The covalent conjugation of DPPE lipid molecules with MWCNTs was confirmed using a Vertex 80 FTIR spectrometer (Bruker, Germany). Infrared spectra were recorded at 2 cm^{-1} resolution at room temperature over a wavenumber range of 1000–4000 cm^{-1}. A ZnSe window was used for recording of IR spectra of all samples. To obtain the IR absorption of samples, COOH-MWCNTs were dispersed in dimethyl sulfoxide (DMSO), and DPPE and MWCNT-lipid conjugate solutions were prepared in chloroform. Samples were observed directly in the ZnSe liquid cell. Spectra of neat solvents were background-subtracted from sample spectra.

Liquid-Liquid Extraction

To confirm the successful conjugation of DPPE with MWCNTs in the carbodiimide-mediated reaction, lipid-modified MWCNTs were dispersed in a vessel containing 2 mL of chloroform and 2 mL of pure water, shaken very well for 10 min and left for an hour to partition into either the chloroform or the water phase.

Lipid Bilayer Fabrication

To form a lipid bilayer on lipid-modified MWCNTs, a solution of 2 mg DPPC in chloroform was mixed with 50 μL DPPE-MWCNT dispersion as prepared in chloroform at total volume of 1 mL. 1 wt% of either tail-labeled NBD-PC or headgroup-labeled NBD-PE was mixed with the DPPC as a fluorescence probe. Chloroform was evaporated under an argon flow and the resulting MWCNT-lipid film was dried in vacuum at room temperature for 3 h to remove any trace of chloroform. 1 mL of 10 mM phosphate buffer, pH 7.5, containing 150 mM NaCl was added to the MWCNT-lipid film and sonicated for 30 min in a bath sonicator. To remove excess lipid from the sonicated suspension of lipid-coated MWCNTs, it was centrifuged for 10 min at 3500 g, the supernatant was discarded, and the nanotubes were resuspended in fresh buffer. Nanotubes were observed using fluorescence confocal microscopy.

Protein Incorporation in Lipid Bilayer-coated Nanotubes

To observe insertion of α-hemolysin into the lipid bilayer with fluorescence confocal microscopy, α-hemolysin from *Staphylococcus aureus* (Sigma) was labeled with NHS-rhodamine. 250 μL of 0.5 mg/mL protein solution in 50 mM sodium bicarbonate buffer, pH 8.5, was incubated with a 5× molar excess of NHS-rhodamine for 2 h at room temperature. To remove excess dye, the reaction mixture was centrifuged using Zeba spin desalting column with 7K MWCO (Thermo Scientific, Pierce). 1 μM labeled α-hemolysin solution was then added to the lipid bilayer-coated MWCNT suspension and incubated at 37°C for 1 h. Unbound α-hemolysin molecules were removed by centrifugation of the suspension for 10 min at 3500 g and resuspension of the resulting nanotube-containing pellet. As control experiments, 1 μM labeled α-hemolysin was incubated with a MWCNT-COOH suspension in PBS buffer or a MWCNT-COOH suspension in PBS buffer with 2.5 mg/mL lyso-PC and mixed well for 1h at 37°C. Free α-hemolysin molecules were removed by centrifugation as described above.

Sample Observation with Fluorescence Confocal Microscopy

To observe MWCNTs, we used a Nikon TI-E inverted microscope (Tokyo, Japan) equipped with a Yokagawa CSUX confocal head (Tokyo, Japan). All images were taken using a 60× oil-immersion objective (Apo TIRF). NBD and rhodamine were excited with 50 mW solid-state lasers at 491 nm and 561 nm, respectively, and the emission signals were recorded at 535 and 595 nm. The suspension of nanotubes was transferred into a Sykes-Moore microscopy chamber (Bellco, Vineland, NJ) containing a #1 glass coverslip. Prior to use, coverslips were first sonicated in 80°C Millipore water for 30 min and then immersed in pure sulfuric acid for 2 h. After rinsing with water thoroughly, coverslips were sonicated in water for 30 min and then sonicated in methanol for 15 min. Cleaned coverslips were dried in a 60°C oven.

Fluorescence Quenching

To confirm the formation of true lipid bilayers on MWCNTs, the total fluorescence of lipid bilayers labeled with 1 wt% of either tail-labeled NBD-PC or head-labeled NBD-PE was measured using a spectrofluorophotometer (RF-5301 PC, Shimadzu, Japan). The samples were excited at 460 nm, and emission signals were recorded at 530 nm. Then, 20 μL of 1 M sodium dithionite in 10 mM PBS buffer with pH 9, prepared fresh and purged with argon, was added to each suspension. One minute after addition of sodium dithionite, the fluorescence of each sample was measured and compared with the initial fluorescence value. Additional aliquots of quencher were then added to the suspension to confirm that no further decrease in fluorescence intensity could be observed, and then, SDS surfactant was added to

the suspension to lyse the membrane and expose the inner leaflet of the bilayer to the quencher.

Transmission Electron Microscopy (TEM)

Thirty microliters of MWCNT suspension in water and 30 μL of lipid bilayer-coated MWCNT suspension in 10 mM phosphate buffer, pH 7.5 were pipetted on paraffin wax surfaces separately. Formvar coated-copper grids (TED Pella, Redding, CA) were placed on the sample droplets for 3–4 minutes and the excess fluid was removed by filter paper. TEM images were taken with a JEOL JEM-2100 LaB6 microscope operating at 200 KV.

Fluorescence Anisotropy Measurements

To verify the fluidity of lipid bilayers bound to the surface of MWCNTs, the fluorescence anisotropy of NBD-labeled DPPC included in the lipid bilayer was measured as a function of temperature using a QuantaMaster QM-4SE spectrofluorometer from PTI (Photon Technology International, Birmingham, NJ, USA). A temperature range of 4–55°C was examined, allowing for the gel-to-liquid phase transition of DPPC to be observed. To equilibrate the cuvette temperature after each temperature change, it was incubated at the target temperature for 30 min, and a pair of measurements was taken to confirm no changes in fluorescence anisotropy. Excitation was at 460 nm and emission was measured at 530 nm.

The sample containing the fluorophore probe was excited with linearly polarized light and the intensities of the vertical and horizontal components of the emitted light were measured to calculate anisotropy (r) using the following equation:

$$r=(I_{VV}-GI_{VH})/(I_{VV}+2GI_{VH})$$

where I_{VV} and I_{VH} are the emitted intensities polarized parallel and perpendicular to the excitation light when the excitation light is polarized vertically. G is a correction factor defined as $G = I_{HV}/I_{HH}$ where I_{HV} and I_{HH} are vertical and horizontal fluorescence emission intensities when the excitation light is polarized horizontally.

RESULTS AND DISCUSSION

Due to the hydrophobic nature of carbon nanotubes, lipid molecules can self-assemble on the nanotube surface via hydrophobic-hydrophobic interactions. This self-assembly, however, does not lead to formation of a lipid bilayer. To fabricate a membrane-like bilayer on a nanotube surface, we covalently conjugated 1, 2-dipalmitoyl-*sn*-glycero-3-phosphoethanolamine (DPPE), a lipid bearing a primary amine on its head group, with COOH-functionalized MWCNTs in a carbodiimide-mediated reaction using *N, N′*-diisopropylcarbodiimide (DIC) (Scheme 1). N-Hydroxysuccinimide (NHS) was added to the reaction mixture to increase the stability of the active reaction intermediate.[50] Since single-walled carbon nanotubes (SWCNTs), with outer diameters of approximately 1–2 nm, are too highly curved to support the formation of closed shell lipid bilayers (the smallest reported inner radius for lipid bilayers is about 5 nm),[14, 46] MWCNTs with diameters in the range of 20–30 nm were used. MWCNTs have some advantages for covalent modification. They have higher mechanical stability than SWCNTs, and since conjugation occurs only on the external walls of the multi-walled nanotubes, the mechanical and electronic properties of the inner walls are unaffected by conjugation.[51]

Solubility of Lipid-modified MWCNTs

To confirm that covalent modification of water-dispersible COOH-functionalized MWCNTs with DPPE converts them into a species that can be dispersed in nonpolar solvents, liquid-liquid extraction of lipid-modified MWCNTs was performed between chloroform and water. The excellent dispersibility of lipid-MWCNT conjugates in chloroform is convincing evidence for the successful conjugation of lipid to MWCNT surfaces (Figure 1). A control experiment in the absence of DIC and NHS resulted in partitioning of the nanotubes to the water phase, confirming lack of any covalent bond between lipids and MWCNTs. A comparison between extraction results for COOH-MWCNTs as supplied by the vendor (Figure 1A), MWCNTs treated with lipids without DIC (Figure 1B) and lipid-conjugated MWCNTs (Figure 1C) clearly establishes the covalent conjugation of lipids to the nanotube surface. The nanotubes in Figures 1A and 1B partition to the water phase due to hydrophilic nature of carboxylic acid group on the oxidized MWCNTs. Covalently modified nanotubes were stable in chloroform and no aggregation was observed even after 3 months.

Our results contrast those of He et al., who reported that lipid-modified CNTs are dispersible in both chloroform and water.[43, 44] We observed similar behavior in CNTs immediately after covalent modification, but when these CNTs were treated with surfactant to remove physisorbed lipid species, they partitioned exclusively to the chloroform phase, as described above. These hydrophobic-surface CNTs, modified with a single layer of lipids, serve as the basis of our bilayer fabrication technique (see Figure 2).

FTIR Spectroscopy

In order to further confirm the reaction between MWCNTs and lipid molecules, Fourier Transform Infrared (FTIR) spectra of a COOH-functionalized MWCNT suspension, DPPE solution, and DPPE-MWCNT conjugate suspension were analyzed. As can be seen in Figure 3, there is a sharp peak at 1662 cm^{-1} in the COOH-functionalized MWCNT IR spectrum (Figure 3A) corresponding to the carboxylate group (COO^{-}) of deprotonated COOH, as reported previously by Singh et al.[27] The peaks at 1989 and 2149 cm^{-1} are indicative of aromatic combination bands of carbon nanotubes.[52] The strong peak at 3475 cm^{-1} in this spectrum corresponds to the hydroxyl (OH) stretch of COOH-MWCNTs. The DPPE spectrum (Figure 3B) shows peaks at 2855 and 2927 cm^{-1} for C-H stretch vibrations in the alkyl chain of saturated lipid tails.[52] Other peaks at 1737 and 1056 cm^{-1} in this spectrum can be attributed to the N-H bend vibration of the primary amine group of DPPE and C-N stretch vibration of the same group in the DPPE, respectively. In the lipid-MWCNT conjugate spectrum (Figure 3C), the two new peaks at 3008 and 1653 cm^{-1} correspond to N-H and C=O vibration of an amide bond. This clearly confirms the formation of covalent amide bonds between DPPE and COOH-functionalized MWCNTs. These two peaks are only seen in the conjugate spectrum. This result for amide peak frequency is in good agreement with result of Singh et al. for formation of an amide bond between a peptide nucleic acid and SWCNTs.[27] Disappearance of the primary amine peak and hydroxyl peak in the conjugate spectrum is verifying evidence for conversion of the lipid primary amine and carboxylic acid to an amide. Appearance of a peak at 1262 cm^{-1} in the lipid-MWCNT conjugate spectrum also corresponds to the C-N stretch vibration of secondary amine of amide bond, and the peaks in the range of 2800–2960 cm^{-1} are indication of the C-H stretch vibration of the conjugated lipid alkyl chain. The peaks at 3604 and 3693 cm^{-1} in the spectra of both the lipid and lipid-MWCNT conjugate are due to the aqueous nature of sample and existence of non-bonded hydroxyl groups.

Lipid Bilayer Formation on MWCNTs

Formation of lipid bilayers on MWCNTs was accomplished by sonication of the zwitterionic DPPC lipid with DPPE-modified MWCNTs in 10 mM phosphate buffer

containing 150 mM NaCl (pH 7.5). Sonication of lipid-MWCNT conjugates with free lipid molecules is a novel method for the formation of bilayer-coated nanotubes. To visualize the structure of lipid-coated MWCNTs, fluorescently labeled lipid (NBD-PC or NBD-PE) was included in the lipid mixture. Figure 4 shows that the sonicated suspension of MWCNT-lipid conjugates has good dispersibility in buffer solution after the removal of excess lipid, and demonstrates that no nanotube sediment can be observed even after two months. Dispersibility of nanotubes in buffer solution is a strong evidence for fabrication of lipid bilayers on MWCNT surfaces, because liposome-like lipid bilayers are stably suspended in aqueous solutions.[53, 54] Similar behavior has been observed for self-assembled photopolymerized lipid micelles in buffer solution.[33]

Fluorescence confocal images show linear fluorescent features in buffer solution corresponding to the lipid bilayer coated-MWCNTs (Figure 5). Since the diameter of MWCNTs used in this study was in the range of 20–30 nm, this result is in good agreement with report of Roiter et al. in which lipid bilayers can easily envelop nanoparticles diameters greater than 22 nm.[55] Moreover, the cylindrical geometry of double-chained phospholipids like DPPC means they easily form lamellar bilayers[36, 56] and adapt to the curvature of 1D nanotubes.[32]

The structure of COOH-functionalized and lipid bilayer-coated MWCNTs was also investigated with transmission electron microscopy (TEM). As shown in Figure 6, COOH-functionalized MWCNTs have a tubular shape, and they are entangled (Figure 6A), while the lipid-coated MWCNTs are more loosely associated and their length is shorter compared to COOH-functionalized nanotubes (Figures 6B, C). The walls of MWCNTs are clearly observed in Figures 6D and 6E. Although there is no major difference in morphology between COOH-functionalized and lipid bilayer-coated MWCNTs, the shorter length and improved dispersion confirms the modification and coating of nanotube surface with a lipid bilayer. Shortening of nanotubes in a carbodiimide-mediated reaction has been reported earlier.[31]

To confirm the formation of true lipid bilayers rather than multilayers on MWCNTs after sonication, two experiments performed. In one experiment, α-hemolysin was inserted into lipid-coated MWCNTs; in another, fluorescence from one leaflet of the lipid bilayer was selectively quenched.

Alpha-hemolysin Insertion in Lipid Bilayers on Nanotube Surfaces

The α-hemolysin protein inserts spontaneously into lipid bilayers, forming heptameric pores through which ions and small molecules can pass.[57–59] Spontaneous insertion of α-hemolysin into the lipid structures on the surface of our modified MWCNTs is evidence that these lipid structures are true molecular bilayers. Alpha-hemolysin from *Staphylococcus aureus* labeled with rhodamine was added to the lipid bilayer-coated MWCNT solution and incubated for 1 h (Figure 2). The images obtained from fluorescence confocal microscopy with excitation at 561 nm and emission at 595 nm confirmed the insertion of rhodamine-labeled α-hemolysin in the lipid membrane (Figure 7). Overlaying images of rhodamine and NBD fluorescence emission clearly shows that α-hemolysin is exactly co-localized with lipid-coated MWCNTs (Figure 7C). In a control experiment, COOH-functionalized MWCNTs with no lipid on them were incubated with labeled α-hemolysin. No α-hemolysin adsorbed to nanotube surfaces (Figure 7D) in the absence of a lipid bilayer. In another control experiment, COOH-functionalized MWCNTs were mixed with lysophosphatidylcholine (lyso-PC), a single-chain lipid with a polar headgroup, in PBS buffer (pH 7.5), and then incubated with labeled α-hemolysin. In this control, a small number of MWCNTs in suspension colocalized with a low level of α-hemolysin fluorescence, demonstrating weak non-specific adsorption (Figure 7E). Lyso-PC molecules

can self-assemble on the surface of carbon nanotubes as a monolayer forming a micelle-like surface, but they cannot form membrane-like bilayers because of their conical molecular shape and curvophilicity.[4, 36] These results show that α-hemolysin interacts only weakly with this lipid monolayer. Together, these observations indicate that the lipids assembled on the surface of MWCNT by covalent conjugaction and sonication form a molecular bilayer rather than a monolayer or disorganized structure.

Lipid Bilayer Fluorescence Quenching

In a complementary experiment, we confirmed the formation of lipid bilayers on MWCNTs by fluorescence quenching. In this experiment, sodium dithionite, which can quench the NBD fluorescence by chemically reducing the dye, was added to a suspension of lipid bilayer-coated MWCNTs in which 1 wt% of either the lipid tails or lipid headgroups were labeled with NBD. As McIntyre and Sleight have shown previously, the reaction of NBD with dithionite results in reduction of the nitro group to an amine without any side reactions or ring opening.[60] This reduction reaction is irreversible and makes NBD nonfluorescent.[61] One minute following quencher addition to the suspensions, a 55.42% (head-labeled) or 47.53% (tail-labeled) decrease in total fluorescence intensity was observed (Figure 8). Dithionite is a charged molecule (dithionite anion) and has very low permeability across lipid bilayers [62]; therefore, it can only quench the fluorescence of lipid molecules placed in the outer leaflet of the bilayer. No further decrease in fluorescence intensities was observed upon addition of more quencher to the suspensions. Upon addition of 10 mM SDS to the suspension, the fluorescence signal immediately dropped to near zero due to exposure of the inner leaflet of the bilayer to the quencher. This observation demonstrates that the initial drop (about 50%) in fluorescence is due to the quenching of the outer leaflet and that the lipid molecules on the MWCNTs take on a molecular bilayer structure. Other reports have demonstrated this technique as a confirmation of the bilayer nature of lipid membranes.[61, 63–65]

Lipid Bilayer Fluidity

Since lipid bilayer fluidity has an important influence on membrane functionality, we confirmed fluidity of our MWCNT-anchored membranes by measuring fluorescence anisotropy (r) of NBD-PC in these membranes as a function of temperature. Fluorescence anisotropy has long been used as a measure of membrane fluidity; as molecular motions are constrained in low-fluidity conditions (e.g. gel phase), fluorescence anisotropy increases.[66–68] A true lipid bilayer would be expected to demonstrate a significant change in fluidity at the lipid gel-to-liquid phase transition. Therefore, we measured fluorescence anisotropy from temperatures across the phase transition temperature of DPPC (~41 °C)[68]. Figure 9 shows the effect of temperature on the fluorescence anisotropy of bilayer-coated MWCNTs. As expected, anisotropy values decrease from 4 °C to 55 °C as lipid rotational motion increases. A drastic change in fluorescence anisotropy can be observed near the expected phase transition temperature of DPPC. This change verifies the fluidity of the bilayers near physiological temperatures and the mobility of lipids within the bilayers.

CONCLUSIONS

The need for biocompatible nanotube-based materials, which have potential applications in biosensing and in energy-producing devices, motivated us to make lipid bilayer-coated MWCNTs. Bilayers are formed in a two-step process. First, DPPE is covalently anchored to the surface of COOH-functionalized MWCNTs in a carbodiimide-mediated reaction. These lipid-modified MWCNTs then serve as a substrate for lipid bilayer assembly via co-sonication with DPPC. Modification of MWCNTs with a covalently anchored bilayer of lipids was confirmed by liquid-liquid extraction, FTIR, fluorescence microscopy, and

differential fluorescence quenching. Lipid bilayer fluidity was verified with fluorescence anisotropy measurements. We also demonstrated that the membrane protein α-hemolysin can spontaneously insert into the bilayers on the MWCNT surfaces. Lipid bilayers can provide a biomimetic environment for integrating proteins with carbon nanotubes, leading to a broad range of analytical and bioelectronic applications.

Acknowledgments

This work was funded in part by the National Institutes of Health under award 1R21AG033890. Fluorescence anisotropy measurements were performed at the NanoBiophysics Core Facility at USC.

References

1. Artyukhin AB, Bakajin O, Stroeve P, Noy A. Layer-by-Layer electrostatic self-assembly of polyelectrolyte nanoshells on individual carbon nanotube templates. Langmuir. 2004; 20:1442–1428. [PubMed: 15803732]
2. Baughman RH, Zakhidov AA, de Heer WA. Carbon nanotubes--the route toward applications. Science. 2002; 297:787–792. [PubMed: 12161643]
3. Dresselhaus, MS.; Dresselhaus, G.; Avouris, P. Carbon nanotubes: synthesis, structure, properties, and applications. Springer; London: 2001.
4. Richard C, Balavoine F, Schultz P, Ebbesen TW, Mioskowski C. Supramolecular self-assembly of lipid derivatives on carbon nanotubes. Science. 2003; 300:775–778. [PubMed: 12730595]
5. Gruner G. Carbon nanotube transistors for biosensing applications. Anal Bioanal Chem. 2006; 384:322–335. [PubMed: 16132132]
6. Heller I, Janssens AM, Mannik J, Minot ED, Lemay SG, Dekker C. Identifying the mechanism of biosensing with carbon nanotube transistors. Nano Lett. 2008; 8:591–595. [PubMed: 18162002]
7. Kam NW, Dai H. Carbon nanotubes as intracellular protein transporters: generality and biological functionality. J Am Chem Soc. 2005; 127:6021–6026. [PubMed: 15839702]
8. Kong J, Franklin NR, Zhou CW, Chapline MG, Peng S, Cho KJ, Dai HJ. Nanotube molecular wires as chemical sensors. Science. 2000; 287:622–625. [PubMed: 10649989]
9. Polizu S, Savadogo O, Poulin P, Yahia L. Applications of carbon nanotubes-based biomaterials in biomedical nanotechnology. J Nanosci Nanotechnol. 2006; 6:1883–1904. [PubMed: 17025102]
10. Shim M, Kam NWS, Chen RJ, Li YM, Dai HJ. Functionalization of carbon nanotubes for biocompatibility and biomolecular recognition. Nano Lett. 2002; 2:285–288.
11. Wang J. Carbon-nanotube based electrochemical biosensors: A review. Electroanalysis. 2005; 17:7–14.
12. Kam NWS, Jessop TC, Wender PA, Dai HJ. Nanotube molecular transporters: Internalization of carbon nanotube-protein conjugates into mammalian cells. J Am Chem Soc. 2004; 126:6850–6851. [PubMed: 15174838]
13. Lei JP, Ju HX. Nanotubes in biosensing. Wiley Interdiscip Rev Nanomed Nanobiotechnol. 2010; 2:496–509. [PubMed: 20803683]
14. Artyukhin AB, Shestakov A, Harper J, Bakajin O, Stroeve P, Noy A. Functional one-dimensional lipid bilayers on carbon nanotube templates. J Am Chem Soc. 2005; 127:7538–7542. [PubMed: 15898805]
15. Huang SC, Artyukhin AB, Misra N, Martinez JA, Stroeve PA, Grigoropoulos CP, Ju JW, Noy A. Carbon nanotube transistor controlled by a biological ion pump gate. Nano Lett. 2010; 10:1812–1816. [PubMed: 20426455]
16. Chen J, Liu HY, Weimer WA, Halls MD, Waldeck DH, Walker GC. Noncovalent engineering of carbon nanotube surfaces by rigid, functional conjugated polymers. J Am Chem Soc. 2002; 124:9034–9035. [PubMed: 12148991]
17. Islam MF, Rojas E, Bergey DM, Johnson AT, Yodh AG. High weight fraction surfactant solubilization of single-wall carbon nanotubes in water. Nano Lett. 2003; 3:269–273.
18. Kahn MGC, Banerjee S, Wong SS. Solubilization of oxidized single-walled carbon nanotubes in organic and aqueous solvents through organic derivatization. Nano Lett. 2002; 2:1215–1218.

19. Moore VC, Strano MS, Haroz EH, Hauge RH, Smalley RE, Schmidt J, Talmon Y. Individually suspended single-walled carbon nanotubes in various surfactants. Nano Lett. 2003; 3:1379–1382.
20. Zhang ZX, Che YK, Smaldone RA, Xu MA, Bunes BR, Moore JS, Zang L. Reversible Dispersion and Release of Carbon Nanotubes Using Foldable Oligomers. J Am Chem Soc. 2010; 132:14113–14117. [PubMed: 20849076]
21. Tu XM, Manohar S, Jagota A, Zheng M. DNA sequence motifs for structure-specific recognition and separation of carbon nanotubes. Nature. 2009; 460:250–253. [PubMed: 19587767]
22. Yurekli K, Mitchell CA, Krishnamoorti R. Small-angle neutron scattering from surfactant-assisted aqueous dispersions of carbon nanotubes. J Am Chem Soc. 2004; 126:9902–9903. [PubMed: 15303847]
23. Baker SE, Cai W, Lasseter TL, Weidkamp KP, Hamers RJ. Covalently bonded adducts of deoxyribonucleic acid (DNA) oligonucleotides with single-wall carbon nanotubes: Synthesis and hybridization. Nano Lett. 2002; 2:1413–1417.
24. Bianco A, Kostarelos K, Partidos CD, Prato M. Biomedical applications of functionalised carbon nanotubes. Chem Commun (Camb). 2005; 5:571–577. [PubMed: 15672140]
25. Hazani M, Naaman R, Hennrich F, Kappes MM. Confocal fluorescence imaging of DNA-functionalized carbon nanotubes. Nano Lett. 2003; 3:153–155.
26. Huang WJ, Taylor S, Fu KF, Lin Y, Zhang DH, Hanks TW, Rao AM, Sun YP. Attaching proteins to carbon nanotubes via diimide-activated amidation. Nano Lett. 2002; 2:311–314.
27. Singh KV, Pandey RR, Wang X, Lake R, Ozkan CS, Wang K, Ozkan M. Covalent functionalization of single walled carbon nanotubes with peptide nucleic acid: Nanocomponents for molecular level electronics. Carbon. 2006; 44:1730–1739.
28. Tasis D, Tagmatarchis N, Georgakilas V, Prato M. Soluble carbon nanotubes. Chemistry. 2003; 9:4000–4008. [PubMed: 12953186]
29. Zhu J, Kim JD, Peng HQ, Margrave JL, Khabashesku VN, Barrera EV. Improving the dispersion and integration of single-walled carbon nanotubes in epoxy composites through functionalization. Nano Lett. 2003; 3:1107–1113.
30. Pham TA, Son SM, Jeong YT. Water-dispersible multi-walled carbon nanotubes and novel hybrid nanostructures. Synth React Inorg Met-Org Nano-Metal Chem. 2010; 40:216–224.
31. Huang WJ, Lin Y, Taylor S, Gaillard J, Rao AM, Sun YP. Sonication-assisted functionalization and solubilization of carbon nanotubes. Nano Lett. 2002; 2:231–234.
32. Noy A, Artyukhin AB, Misra N. Bionanoelectronics with 1D materials. Mater Today. 2009; 12:22–31.
33. Contal E, Morere A, Thauvin C, Perino A, Meunier S, Mioskowski C, Wagner A. Photopolymerized lipids self-assembly for the solubilization of carbon nanotubes. J Phys Chem B. 114:5718–5722. [PubMed: 20380427]
34. Douroumis D, Fatouros DG, Bouropoulos N, Papagelis K, Tasis D. Colloidal stability of carbon nanotubes in an aqueous dispersion of phospholipid. Int J Nanomedicine. 2007; 2:761–766. [PubMed: 18203442]
35. Lin SJ, Keskar G, Wu YN, Wang X, Mount AS, Klaine SJ, Moore JM, Rao AM, Ke PC. Detection of phospholipid-carbon nanotube translocation using fluorescence energy transfer. Appl Phys Lett. 2006; 89:143118.
36. Wu Y, Hudson JS, Lu Q, Moore JM, Mount AS, Rao AM, Alexov E, Ke PC. Coating single-walled carbon nanotubes with phospholipids. J Phys Chem B. 2006; 110:2475–2478. [PubMed: 16471843]
37. Goodwin AP, Tabakman SM, Welsher K, Sherlock SP, Prencipe G, Dai H. Phospholipid-dextran with a single coupling point: a useful amphiphile for functionalization of nanomaterials. J Am Chem Soc. 2009; 131:289–296. [PubMed: 19061329]
38. Zhang LQ, Longo ML, Stroeve P. Mobile phospholipid bilayers on a polyion/alkylthiol layer pair. Langmuir. 2000; 16:5093–5099.
39. Gagner J, Johnson H, Watkins E, Li Q, Terrones M, Majewski J. Carbon nanotube supported single phospholipid bilayer. Langmuir. 2006; 22:10909–10911. [PubMed: 17154562]
40. Huang YX, Palkar PV, Li LJ, Zhang H, Chen P. Integrating carbon nanotubes and lipid bilayer for biosensing. Biosen Bioelectron. 2010; 25:1834–1837.

41. Zhou XJ, Moran-Mirabal JM, Craighead HG, McEuen PL. Supported lipid bilayer/carbon nanotube hybrids. Nat Nanotechnol. 2007; 2:185–190. [PubMed: 18654251]
42. Ye JS, Cui HF, Wen Y, Zhang WD, Ottova A, Tien HT, Xu GQ, Sheu FS. Self-assembly of bilayer lipid membrane at multiwalled carbon nanotubes towards the development of photo-switched functional device. Electrochem Commun. 2005; 7:81–86.
43. He P, Urban MW. Controlled phospholipid functionalization of single-walled carbon nanotubes. Biomacromolecules. 2005; 6:2455–2457. [PubMed: 16153079]
44. He P, Zhu XY. Synthesis and characterization of phospholipid-modified multiwalled carbon nanotubes. Mater Res Bull. 2008; 43:141–148.
45. Gao Y, Kyratzis I. Covalent immobilization of proteins on carbon nanotubes using the cross-linker 1-ethyl-3-(3-dimethylaminopropyl)carbodiimide-a critical assessment. Bioconjugate Chem. 2008; 19:1945–1950.
46. Huang C, Mason JT. Geometric packing constraints in egg phosphatidylcholine vesicles. Proc Natl Acad Sci US A. 1978; 75:308–310.
47. Bakas L, Ostolaza H, Vaz WLC, Goni FM. Reversible adsorption and nonreversible insertion of Escherichia coli alpha-hemolysin into lipid bilayers. Biophys J. 1996; 71:1869–1876. [PubMed: 8889162]
48. Valeva A, Weisser A, Walker B, Kehoe M, Bayley H, Bhakdi S, Palmer M. Molecular architecture of a toxin pore: A 15-residue sequence lines the transmembrane channel of staphylococcal alpha-toxin. EMBO J. 1996; 15:1857–1864. [PubMed: 8617232]
49. Schindel C, Zitzer A, Schulte B, Gerhards A, Stanley P, Hughes C, Koronakis V, Bhakdi S, Palmer M. Interaction of Escherichia coli hemolysin with biological membranes - A study using cysteine scanning mutagenesis. Eur J Biochem. 2001; 268:800–808. [PubMed: 11168421]
50. Hermanson, GT. Bioconjugate techniques. Academic Press; London: 1996.
51. Lamprecht C, Danzberger J, Lukanov P, Tiilmaciu CM, Galibert AM, Soula B, Flahaut E, Gruber HJ, Hinterdorfer P, Ebner A, Kienberger F. AFM imaging of functionalized double-walled carbon nanotubes. Ultramicroscopy. 2009; 109:899–906. [PubMed: 19375857]
52. Meyers, RA. Encyclopedia of analytical chemistry: applications, theory and instrumentation. John Wiley; Chichester: 2000.
53. Basu, SC.; Basu, M. Liposome methods and protocols. Humana Press; Totowa: 2002.
54. Weissig, V.; Torchilin, VP. Liposomes: a practical approach. 2. Torchilin, Vladimir; Weissig, Volkmar, editors. Oxford University Press; Oxford: 2003.
55. Roiter Y, Ornatska M, Rammohan AR, Balakrishnan J, Heine DR, Minko S. Interaction of nanoparticles with lipid membrane. Nano Lett. 2008; 8:941–944. [PubMed: 18254602]
56. Hamai C, Yang TL, Kataoka S, Cremer PS, Musser SM. Effect of average phospholipid curvature on supported bilayer formation on glass by vesicle fusion. Biophys J. 2006; 90:1241–1248. [PubMed: 16299084]
57. Aksimentiev A, Schulten K. Imaging alpha-hemolysin with molecular dynamics: Ionic conductance, osmotic permeability, and the electrostatic potential map. Biophys J. 2005; 88:3745–3761. [PubMed: 15764651]
58. Dinges MM, Orwin PM, Schlievert PM. Exotoxins of Staphylococcus aureus. Clin Microbiol Rev. 2000; 13:16–34. [PubMed: 10627489]
59. Song L, Hobaugh MR, Shustak C, Cheley S, Bayley H, Gouaux JE. Structure of staphylococcal alpha-hemolysin, a heptameric transmembrane pore. Science. 1996; 274:1859–66. [PubMed: 8943190]
60. McIntyre JC, Sleight RG. Fluorescence assay for phospholipid membrane asymmetry. Biochemistry. 1991; 30:11819–11827. [PubMed: 1751498]
61. Kamal MM, Mills D, Grzybek M, Howard J. Measurement of the membrane curvature preference of phospholipids reveals only weak coupling between lipid shape and leaflet curvature. Proc Natl Acad Sci US A. 2009; 106:22245–22250.
62. Moreno MJ, Estronca LMBB, Vaz WLC. Translocation of phospholipids and dithionite permeability in liquid-ordered and liquid-disordered membranes. Biophys J. 2006; 91:873–881. [PubMed: 16617082]

63. Hu PCC, Li S, Malmstadt N. Microfluidic fabrication of asymmetric giant lipid vesicles. ACS Appl Mater Interfaces. 2011; 3:1434–1440. [PubMed: 21449588]

64. Pautot S, Frisken BJ, Weitz DA. Engineering asymmetric vesicles. Proc Natl Acad Sci US A. 2003; 100:10718–10721.

65. Gruber HJ, Schindler H. External surface and lamellarity of lipid vesicles - a practice-oriented set of assay-methods. Biochim Biophys Acta. 1994; 1189:212–224. [PubMed: 8292627]

66. Mesquita R, Melo E, Thompson TE, Vaz WLC. Partitioning of amphiphiles between coexisting ordered and disordered phases in two-phase lipid bilayer membranes. Biophys J. 2000; 78:3019–3025. [PubMed: 10827980]

67. Marczak A. Fluorescence anisotropy of membrane fluidity probes in human erythrocytes incubated with anthracyclines and glutaraldehyde. Bioelectrochemistry. 2009; 74:236–239. [PubMed: 19064336]

68. Lentz BR, Barenholz Y, Thompson TE. Fluorescence depolarization studies of phase-transitions and fluidity in phospholipid bilayers. 1. Single component phosphatidylecholine liposomes. Biochemistry. 1976; 15:4521–4528. [PubMed: 974073]

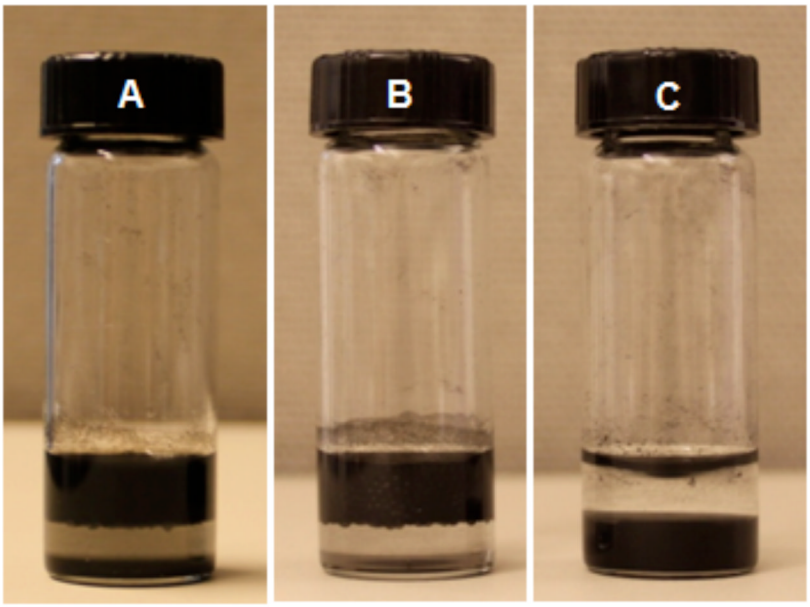

Figure 1.

Liquid-liquid extraction of MWCNTs in a $CHCl_3$/H2O system. The upper phase is water and the lower phase is chloroform. Images show partitioning of MWCNTs to either the chloroform or water phase after shaking the mixtures for 10 min and separating for 1 h. (A) COOH-MWCNTs; (B) A negative control consisting of physically mixed MWCNTs and lipid reagents with no DIC or NHS; (C) Conjugated lipid-MWCNTs from the carbodiimide-mediated reaction. All unbound and physisorbed lipid molecules have been removed by treatment with surfactant. It is clear that MWCNTs in the negative control behave like COOH-functionalized MWCNTs and partition to the water phase, while covalently modified lipid-MWCNTs partition to the chloroform phase.

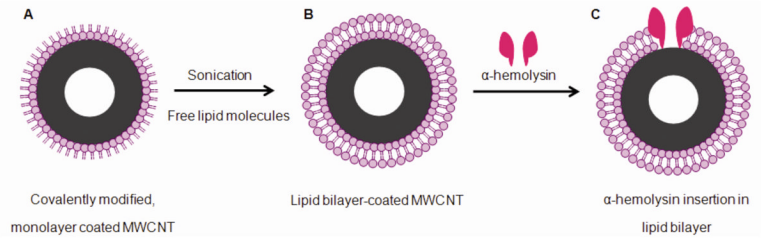

Figure 2.

Schematic drawing of the insertion of protein into the bilayer of a lipid-modified MWCNT (Front view). (A) Covalent modification of a COOH-MWCNT after reaction with DPPE; (B) Lipid bilayer formation during sonication of lipid-modified MWCNT with DPPC molecules in phosphate buffer and (C) insertion of α-hemolysin in the lipid bilayer-coated MWCNT. Drawing not to scale.

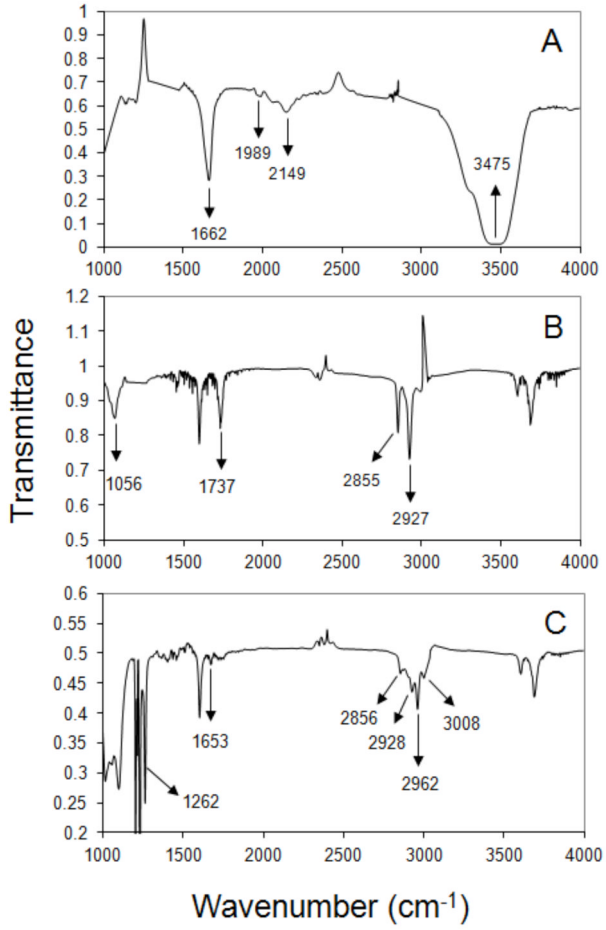

Figure 3.

FTIR spectra of (A) COOH-MWCNTs; (B) DPPE; (C) MWCNT-DPPE conjugate. Appearance of NH stretch (3008 cm^{-1}) and C=O stretch (1653 cm^{-1}) peaks in figure C correspond to amide bond formation, and the disappearance of NH_3^+ and OH peaks in this figure confirms the conversion of primary amine and carboxylic acid to the amide linking the lipid to the MWCNT surface.

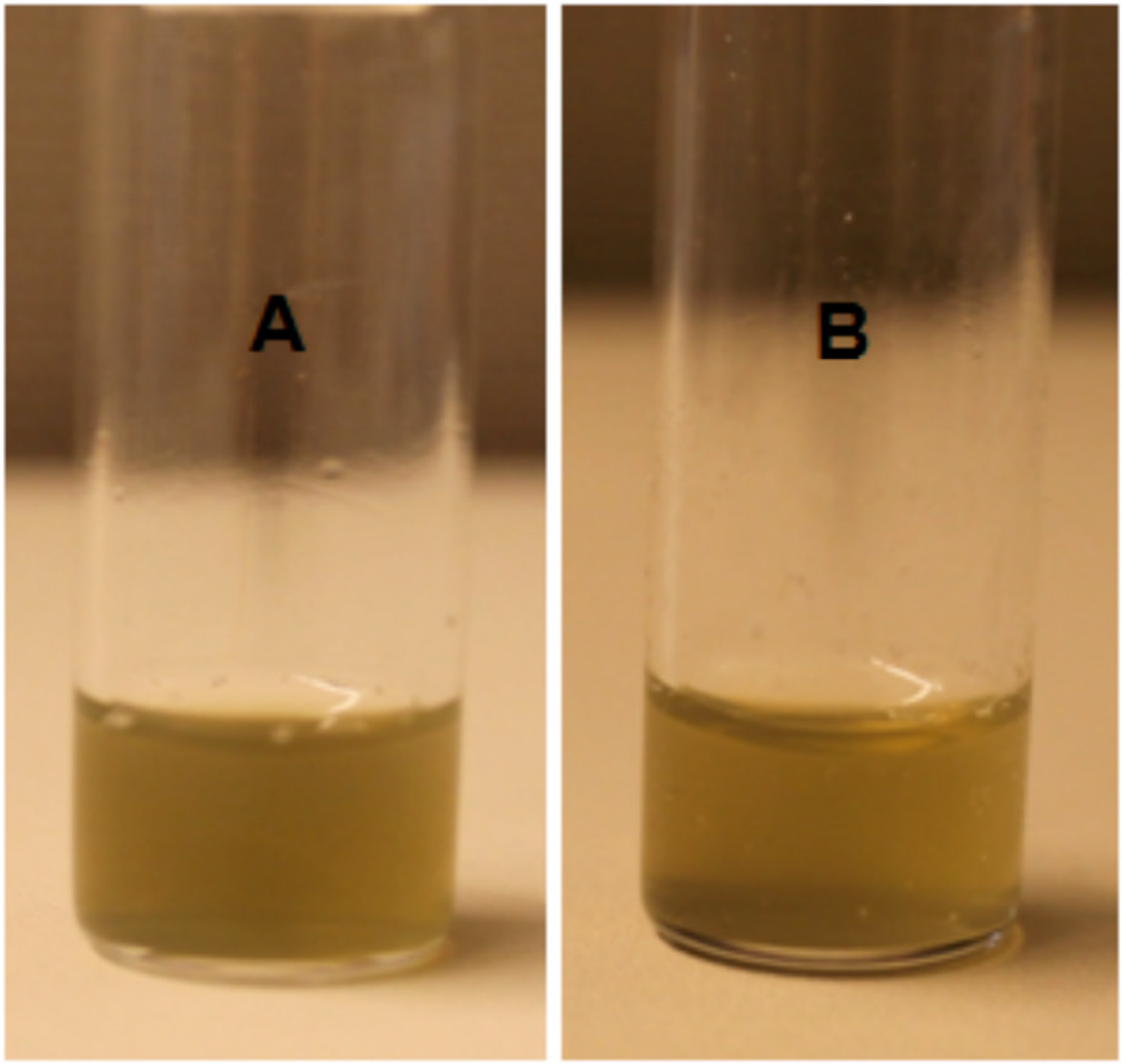

Figure 4.
Photographs of sonicated lipid bilayer-coated MWCNTs in buffer after (A) 1 day, and (B) 60 days. Lipid bilayer-coated MWCNTs are well dispersed in buffer.

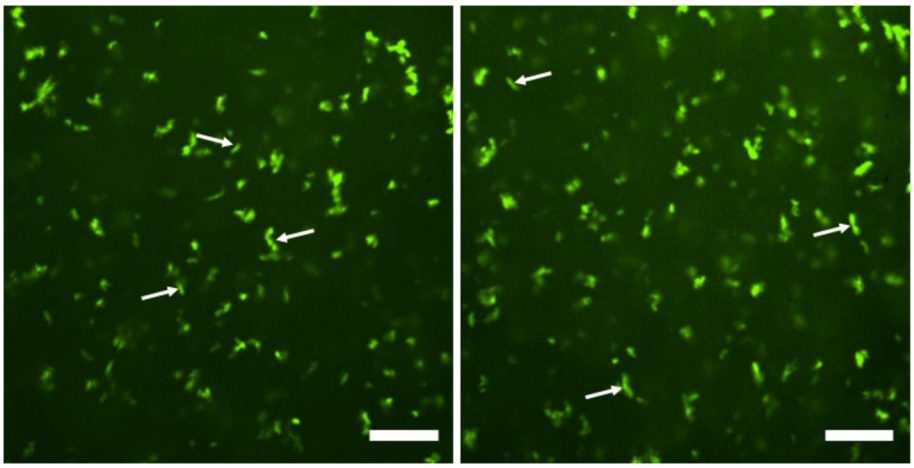

Figure 5.
Confocal images of MWCNTs coated with NBD-DPPC-containing lipid bilayers in buffer solution. Arrows indicate linear nanotubes. Scale bars: 10 μm.

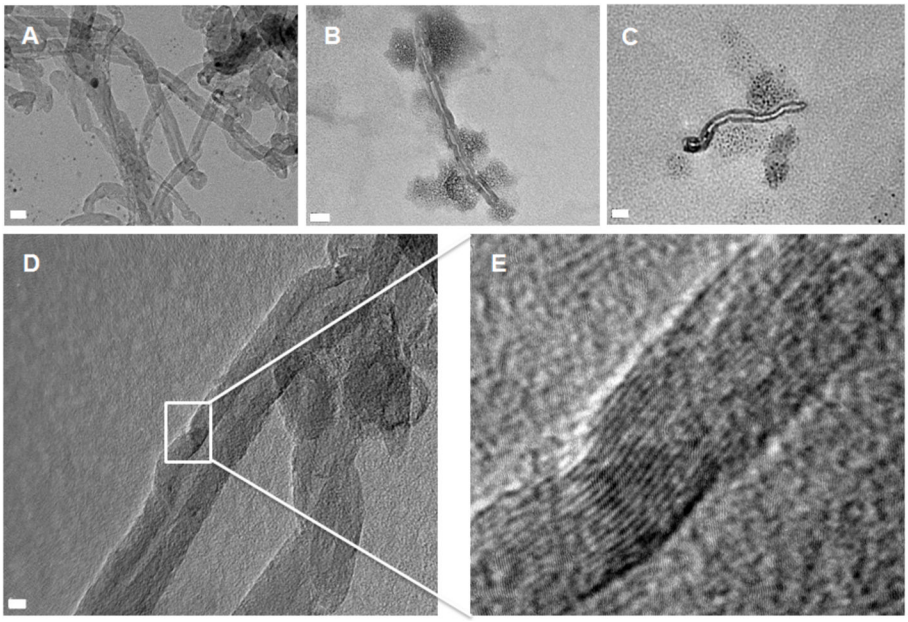

Figure 6.
TEM images of (A) COOH-MWCNTs and (B and C) bilayer-coated MWCNTs after removal of excess lipid. (D) Closer view of COOH-MWCNTs; (E) an enlarged image of part of the nanotube wall. Lipid-coated MWCNTs are shorter than COOH-MWCNTs, and are less tangled. COOH-MWCNTs were deposited from suspension in pure water and lipid-coated MWCNTs were deposited from suspension in phosphate buffer solution. Dark areas in (B) and (C) are salt crystals formed after drying the buffer-containing sample on formvar-coated grids. Scale bars: (A and C) 20 nm; (B) 50 nm; (D) 5 nm; and (E) is an expanded view of the portion of D in the white box.

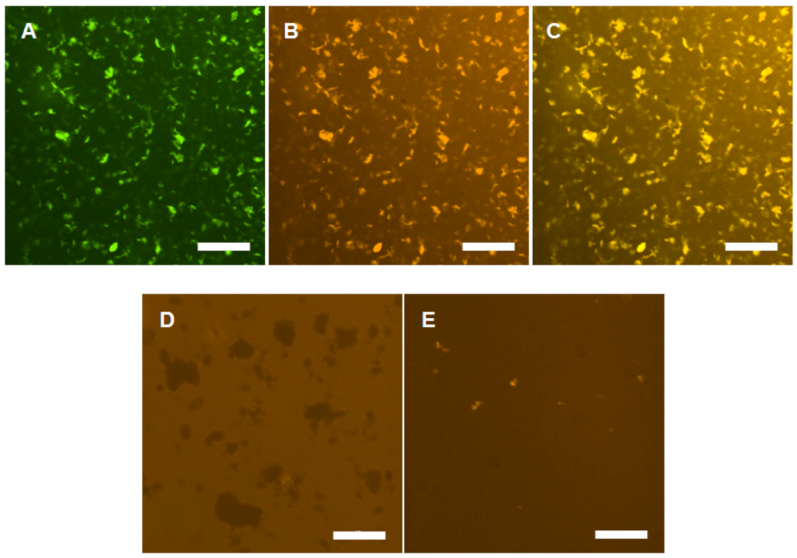

Figure 7.

Confocal fluorescence images of (A) NBD-labeled lipids on MWCNTs coated with lipid bilayers by sonication (ex: 491 nm, em: 535 nm); (B) spontaneous insertion of rhodamine-labeled α-hemolysin after incubation of bilayer-coated MWCNTs with protein at 37°C for 1 h (ex: 561 nm, em: 595 nm); (C) Overlay of figures (A) and (B), which shows colocalization of α-hemolysin with bilayer-coated MWCNTs; (D) COOH-MWCNTs incubated with rhodamin-labeled α-hemolysin (negative control); and (E) COOH-MWCNTs coated with single-chain lyso-PC lipid and incubated with rhodamine-labeled α-hemolysin (negative control). No rhodamine fluorescence emission was observed on MWCNTs in (D). A very low rhodamine fluorescence emission from a few MWCNTs in figure (E) is the result of nonspecific adsorption of α-hemolysin to lipid monolayer-coated MWCNTs. Scale bars: 10 μm.

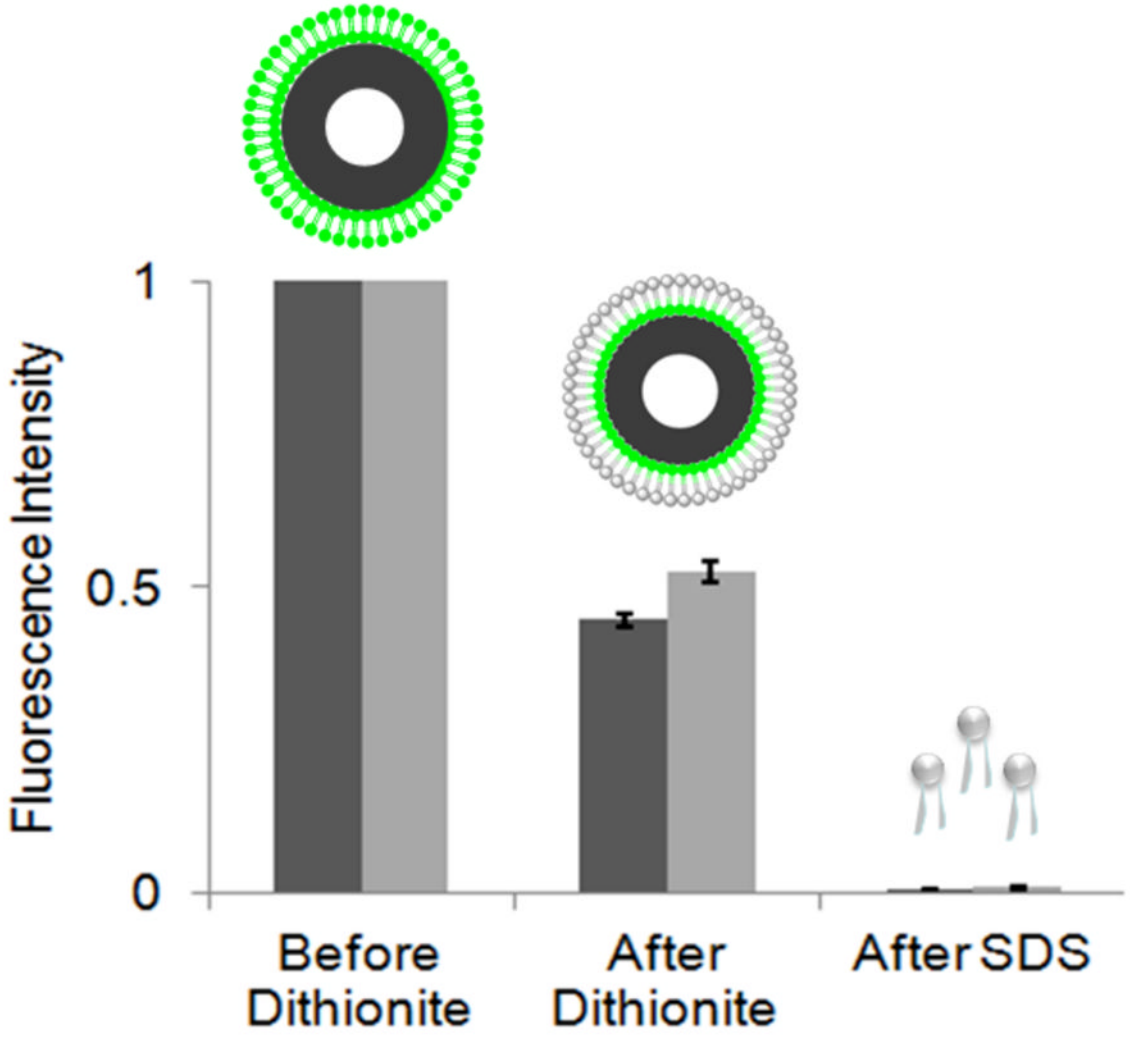

Figure 8.
Normalized fluorescence intensity of bilayer-coated MWCNTs before and after the addition of sodium dithionite quencher. The total fluorescence intensity dropped 55.42% and 47.53% for head-labeled NBD-PE (dark gray) and tail-labeled NBD-PC (light gray), respectively, after addition of quencher. Sodium dithionite only quenches lipid molecules in the outer leaflet of bilayer. Addition of 10 mM SDS surfactant reduced the fluorescence intensities to about zero. These data demonstrate that only half of the lipid population is in the outer leaflet of the bilayer, as expected for a molecular bilayer of lipids.

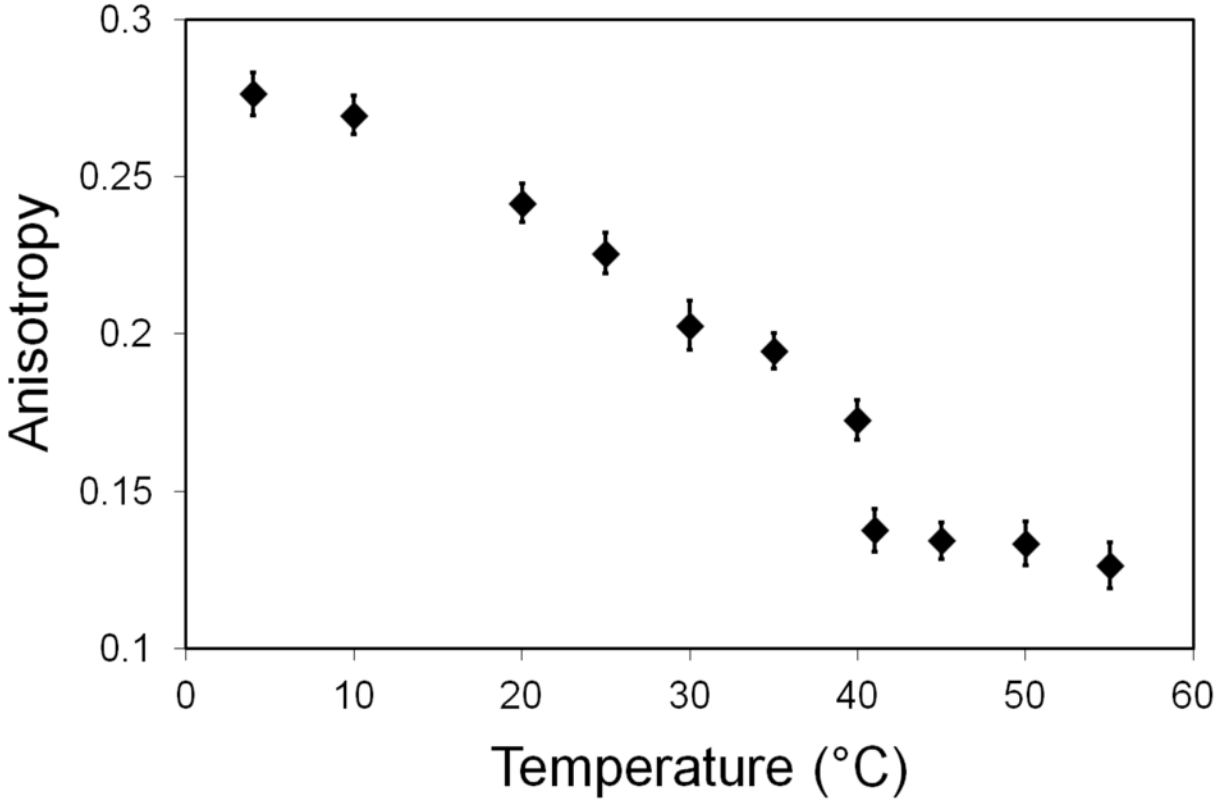

Figure 9.
Fluorescence anisotropy of lipid bilayers conjugated to the surface of MWCNTs as a function of temperature. Decreasing the temperature from 55 to 4 °C results in an increase in fluorescence anisotropy. The gel-to-liquid phase transition is clear at ~40 °C.

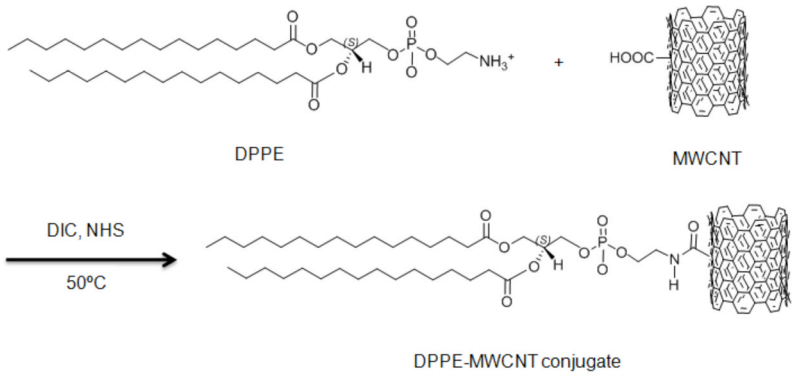

Scheme 1.
Synthesis of lipid-MWCNT conjugates in a carbodimiide-mediated reaction (not to scale).